Biointerface Research in Applied Chemistry
Open-Access Journal (ISSN: 2069-5837)

Article
Volume 13, Issue 4, 2023, 383
https://doi.org/10.33263/BRIAC134.383

Reduced Graphene Oxide/Silica Nanocomposite as Anticancer Drug Delivery Nanocarrier

Akram Khanmohammadi [1], Vahid Rashidi [1], Somayeh Sadighian [1]

[1] Department of Pharmaceutical Biomaterials, School of Pharmacy, Zanjan University of Medical Sciences, Zanjan, Iran
* Correspondence: somayeh.sadighian@gmail.com (S.S.);

Scopus Author ID 26325122200
Received: 30.07.2022; Accepted: 20.09.2022; Published: 31.10.2022

Abstract: This study synthesized a reduced graphene oxide-silica-based (rGO/SiO_2) nanocomposite for quercetin delivery as an anticancer model drug delivery. The synthesized rGO/SiO_2 nanocomposite was investigated by several characterization methods such as Fourier-transform infrared (FT-IR) spectroscopy, X-ray diffraction (XRD) analysis, and Transmission electron microscopy (TEM), and Energy-dispersive X-ray spectroscopy (EDX). The experiments result show that the rGO/SiO_2 nanocomposite has been synthesized successfully and has an average particle size of 50-120 nm.

Keywords: reduced graphene oxide; silica; drug delivery; quercetin.

1. Introduction

Graphene, with vast, fascinating properties such as high mechanical strength, thermal, and electrical properties, and unique optical properties, is a potential applicant for use in several research fields [1]. But, the water-insoluble nature of graphene has limited its applications in biomedical and drug applications. Of course, graphene oxide (GO) and reduced graphene oxide (rGO), which are graphene derivatives and have graphene properties, can disperse in water, which is important for medical and medicine use [2, 3]. Graphene oxide (GO) is a derivative of graphene obtained by the oxidation of graphite, known as Hammer's method [4, 5]. GO is an available and easily scalable material with unique properties such as electronics, energy storage and conversion, biotechnology, and nanocomposite materials. Also, GO has a vast surface area with high oxygen groups such as carboxylic acid, epoxide, and alcohol that let GO be dispersed in water under ultrasonic situations. These factors have led to GO receiving special attention in many applications [6, 7]. Due to the ability of π-π bonds and hydrophobic bonds between GO and aromatic structures, GO has a high capacity to absorb molecules and biological drugs with aromatic structures and has been considered for drug delivery purposes [7, 8]. Some studies have reported that graphene oxide has toxicity in vitro cell culture, and in animal studies, it should be coated on its surface with other nanoparticles [9, 10]. Silica nanoparticles are one of the most hopeful transfer systems agreed upon as nontoxic carriers and are a potential candidate for drug delivery [11-13]. Porous silica nanoparticles have unique properties as drug carriers, such as adjustable pores size, good temperature, chemical stability, and ligand binding capability [14, 15]. So, one of the nanoparticles that can be mounted on graphene oxide sheets and reduce their toxicity is silica compounds.

In this paper, rGO/ SiO_2 nanocomposite was synthesized for the delivery of quercetin as a drug model. Quercetin is an occurring flavonoid present in vegetables, fruits, and tea. The

studies of quercetin have shown several pharmacological activities, such as anti-inflammation, antibacterial, antitumor, and antioxidant, which have the potential to suppress many tumor-related processes [16, 17]. Quercetin, like most flavonoids, is insoluble in water but soluble in ethanol. In addition, the usage of quercetin in pharmaceutical studies is limited due to chemical instability and short biological half-life [18-20]. One approach to overcome this obstacle is to use nanoparticles.

2. Materials and Methods

2.1. Materials and reagents.

Tetraorthosilicates (TEOS, $C_8H_{20}O_4Si$), graphite flakes, quercetin, potassium permanganate ($KMnO_4$), hydrogen peroxide (H_2O_2), potassium bromide (KBr), sodium hydroxide (NaOH) are provided by Merck Company.

2.2. Reduced graphene oxide preparation.

Graphene oxide (GO) was synthesized by Hummer's method [4]. Briefly, 200 mg of black graphite powder was added to 24 ml of concentrated sulfuric acid and stirred in an ice bath for 1 h. Then, 1.2 g $KMnO_4$ was added to the mixing solution and stirred for another 15 min. The mixing solution was transferred to room temperature, and stirring was continued for 24 h. Then the temperature was increased to 100 °C. 30 ml of distilled water was gradually added to the mixture to make sure the excess $KMnO_4$ was removed [21]. 10 ml of distilled water and 5 ml of hydrogen peroxide (H_2O_2) were slowly added to complete the reaction at room temperature. The prepared GO was centrifuged at 8500 rpm for 10 min, washed with 5% HCl solution and deionized water several times, and dried in an oven at 60 ºC for 12 h. The GO was transferred into a Teflon-lined stainless steel autoclave, and the autoclave was done in an oven at 180 ºC for 8 h.

2.3. Preparation of silica-coated reduced graphene oxide.

Silica-coated reduced graphene oxide (rGO/SiO_2) was synthesized using solvothermal. In summary, 100 mg rGO and 1.679 g TEOS were dispersed separately in 10 ml ethanol using sonicate bath. Then two suspensions were mixed and transferred into an oil bath at 40 °C and stirred for 10 min. 0.25 g ammonia was quickly added to the suspension and stirred for 15 h at room temperature. Finally, the rGO/SiO_2 nanocomposite was separated by 8000 rpm centrifugation, washed with distilled water and ethanol several times, and dried in an oven at 60 ºC for 24 h. To achieve the porous nanocomposite, calcination was transferred to an oven at 500 °C for 6 h.

2.4. Preparation of quer-loaded rGO/SiO_2 nanocomposite.

50 mg rGO/SiO_2 were dispersed in 5 mL ethanol under stirring at 500 rpm. 10 mg Quer was dissolved in 5 mL ethanol and then added to the suspension. The mixture was kept stirring for 24 h under dark conditions at room temperature. The Quer-loaded rGO/SiO_2 nanocomposite was collected by centrifugation and washed with distilled water and ethanol to remove the unloaded Quer. Quer-loaded rGO/SiO_2 nanocomposite dried in a vacuum oven at 35 ºC for 12 h.

2.5. Physical loading of quer.

5 mg of rGO/SiO2/Quer were redispersed in 10 mL of ethanol to determine the loading efficiency. Drug loading (DL) and encapsulation efficiency (EE) percentages were calculated by measuring the concentration of Quer in the supernatant by UV-Vis spectrophotometry at a wavelength of 374 nm. Then the amount of DL and EE was calculated using the equation (1) and (2), respectively:

$$\% \text{ DL} = \frac{\text{Weight of drug in nanocomposite}}{\text{weight of nanocomposite}} \times 100 \quad (1)$$

$$\% \text{ EE} = \frac{\text{The total drug} - \text{Free drug}}{\text{The total drug}} \times 100 \quad (2)$$

2.6. In vitro quer release study of rGO/SiO_2 nanocomposite.

The Quer release profile of rGO/SiO_2 nanocomposite was investigated by dialysis bag in phosphate-buffered saline (PBS) solution including 0.5 % tween 80 and adjusted pH (pH 7.4 and 5.4). 5 mg rGO/SiO_2 nanocomposite was put into the dialysis sac (Mw 12 kDa) and immersed in 20 ml of PBS at 37 ºC under a shaker at 150 rpm (SI-1000, Heidolph, Germany). At specified times, 1.0 ml of solution was removed to measure the amount of Qure released using UV-Vis spectroscopy at 374 nm. To maintain the equilibrium of the solution volume, 1.0 mL of fresh buffer solution was added. All studies were performed in three replications.

3. Results and Discussions

3.1. Characterization of the nanocomposite.

3.1.1. FT-IR analysis.

In Figure 1, the broad peak at 3438 cm^{-1} is assigned to stretching vibrations of the hydroxyl group of water. The main characteristic peaks of rGO are shown in figure 1 (A). The peaks at 1421 and 1577 cm^{-1} corresponded to the C=C bond (aromatic group) and C-O (carbonyl and carboxyl moieties) group of rGO, respectively [21, 22].

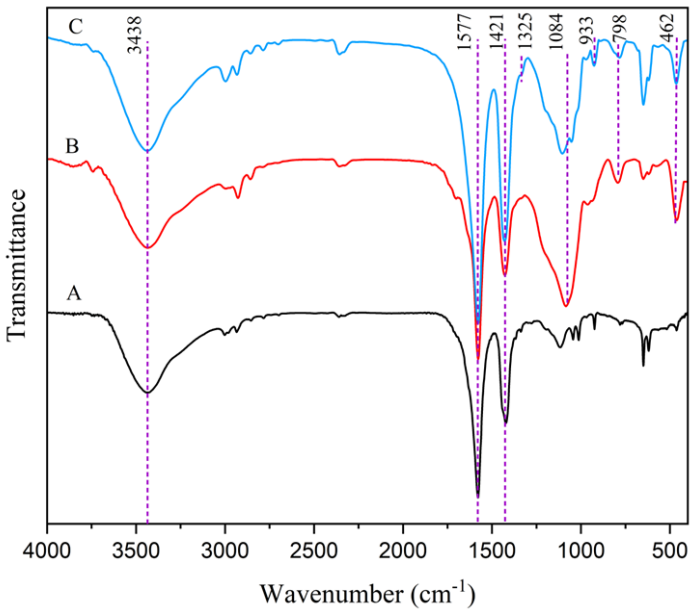

Figure 1. FT-IR spectra of (A) rGO, (B) rGO/SiO_2, and (C) rGO/SiO_2/Quer.

By comparing figures 1 (A) and (B), can be seen new peaks at 1084, 798, and 462 cm^{-1} in the FT-IR spectrum of GO/Si, which is related to asymmetric stretching, symmetric stretching, and vibration modes of Si-O-Si bonds that demonstrate SiO_2 on the surface of rGO sheets. The FT-IR spectrum of rGO/SiO_2/Quer is shown in figure 1 (C). Quer's peaks overlapped with a broad peak at 1084 Si-O-Si bonds, but characteristic bands of Quer were detected. The low-intensity band at 1325 cm^{-1} was attributed to the OH bending of the phenol functions. The out-of-plane bending band of C–H in aromatic hydrocarbon was detectable at 933 cm^{-1}. However, Quer addition caused a slight change in intensity and the downward offset of the Si-O-Si bands; these changes could be due to interactions between the inorganic matrix and the quercetin, which caused variations in bond length, and, thus, bond strength [23, 24].

3.1.2. XRD analysis.

XRD technique was performed to investigate and identify the crystallinity of the structure of rGO/SiO_2 nanoparticles [25]. The rGO/SiO_2 XRD pattern is shown in figure 2. The wide peak at 2Θ: 24.6° is related to rGO, and the widening of the peak can indicate its amorphous structure [26]. The peak of 2° is also related to the structure of mesoporous silica [27].

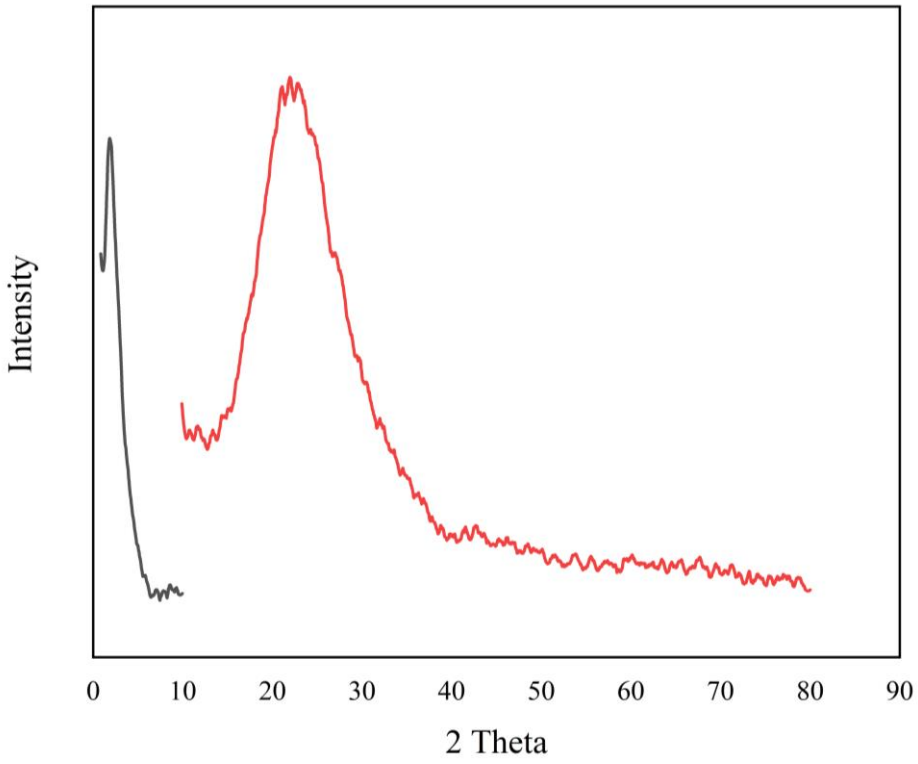

Figure 2. XRD patterns of rGO/SiO_2.

3.1.3. Morphological characterization.

The rGO/SiO2 nanocomposite morphology was investigated via TEM (figure 3). The average particle size is between 70 - 80 nm. As seen in the TEM structure, the structure of rGO and silica are placed together. Silica nanoparticles are visible in a porous form in the TEM image, and reduced graphene oxide nanoparticles can be seen in a smoother form [28, 29].

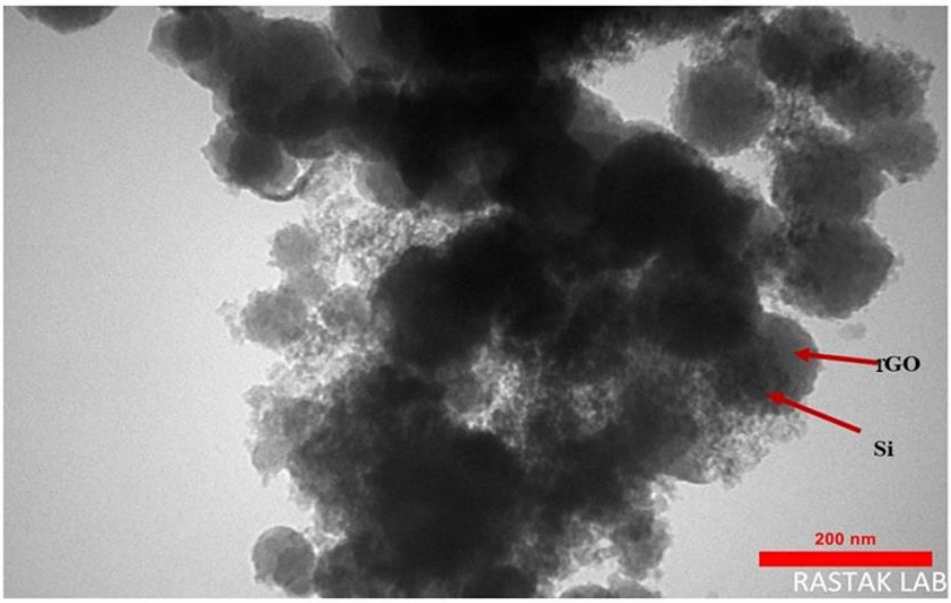

Figure 3. TEM image of rGO/SiO_2 nanocomposite.

3.1.4. EDX analysis.

EDX analysis was used to observe the distribution of silica nanoparticles on rGO layers. It can be seen that SiO_2 nanoparticles have covered almost the entire surface of the rGO layers. The distribution of SiO_2 on the surface of rGO sheets can be seen [30-32].

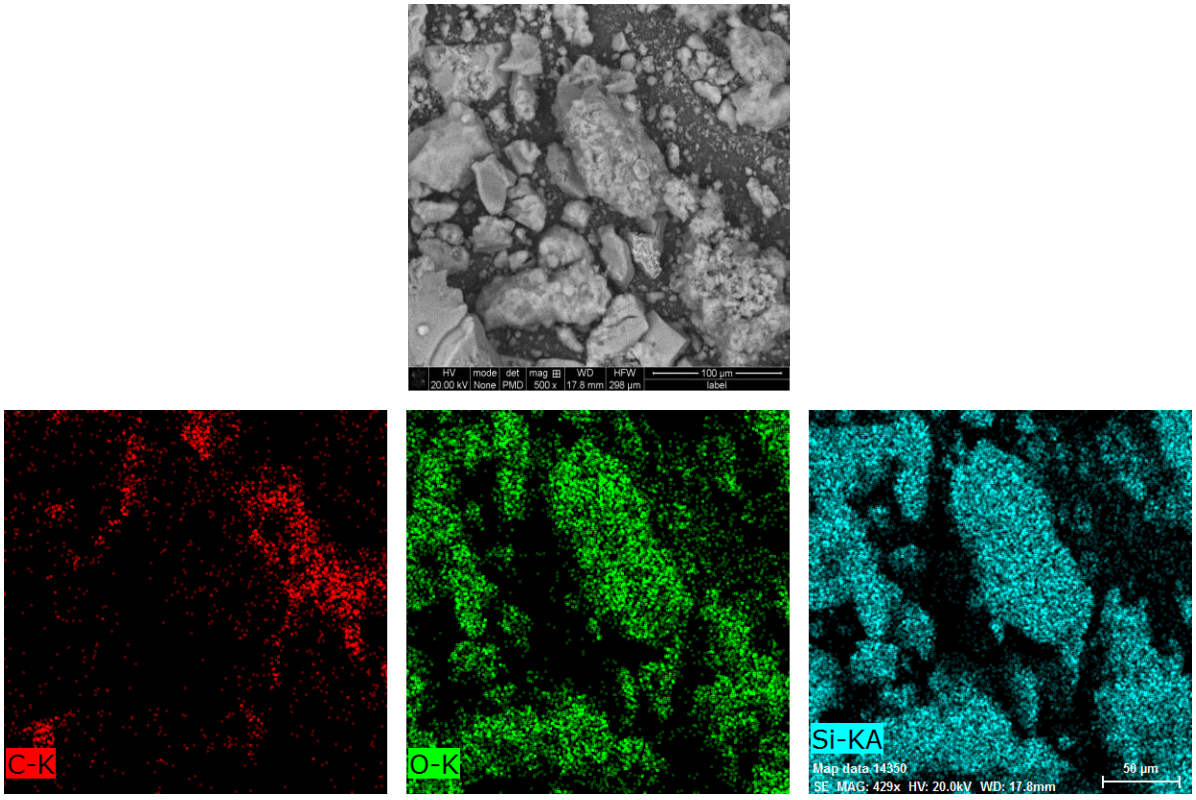

Figure 4. EDX images of rGO/SiO_2 nanocomposite.

3.2. Drug loading and in vitro release study of the drug.

Quer was selected as a model drug for the investigation of DL and release profile of rGO/SiO_2/Quer as a nanocarrier. DL and EE % were calculated at 27 and 60 %, respectively.

In Figure 5, the release profile of Quer from rGO/SiO_2/Quer nanocomposite and free Quer can be seen in natural and acidic conditions (pH 7.4 and 5.4, respectively). As shown in Figure 5, the free drug had a fast release, whereas rGO/SiO_2/Quer nanocomposite is shown a controlled and sustained drug profile. In addition, due to the easier cleavage of the chemical bond between the drug and the nanocomposite in an acidic medium, the amount of release of Quer in an acidic medium is higher than in a neutral medium. Since the environment of cancer cells is acidic, this character of the nanocomposite, rGO/SiO_2 nanocomposite, can be useful for cancer drug delivery [33, 34].

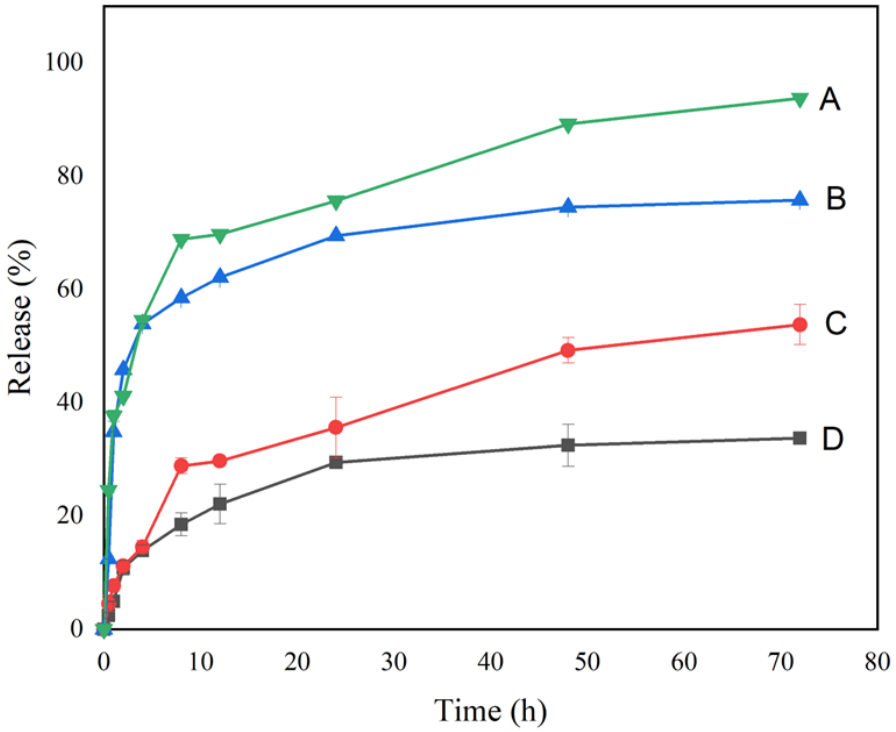

Figure 5. *In vitro* release profile of Quer (A pH 7.4 and B pH 5.5) and rGO/SiO_2/Quer (C pH 7.4 and D pH 5.5). Each data point represents the mean ± S.D. (n = 3).

4. Conclusions

In summary, this project synthesized reduced graphene oxide with silica-coated (rGO/SiO2) as a drug delivery nanocarrier. The release profile of the designed system to deliver quercetin as a drug model was investigated in acidic and neutral environments. The release of acidic pH is greater than in the natural. Consequently, results suggest that rGO/SiO_2 can be a good candidate for the anticancer drug delivery system.

Funding

This research received no external funding.

Acknowledgments

This work was supported by the Zanjan University of Medical Sciences and the University of Zanjan (Grant No. A-12-928-22).

Conflicts of Interest

The authors declare no conflict of interest.

References

1. Verma, A.J.A.S.; Progress, E. A Perspective on the Potential Material Candidate for Railway Sector Applications: PVA Based Functionalized Graphene Reinforced Composite. *Applied Science and Engineering Progress* **2022,** *15*, 5727-5727, http://dx.doi.org/10.14416/j.asep.2022.03.009.
2. Hoseini-Ghahfarokhi, M.; Mirkiani, S.; Mozaffari, N.; Sadatlu, M.A.A.; Ghasemi, A.; Abbaspour, S.; Akbarian, M.; Farjadain, F.; Karimi, M. Applications of graphene and graphene oxide in smart drug/gene delivery: is the world still flat? *Int J Nanomedicine* **2020,** *15*, 9469-9496, https://doi.org/10.2147/ijn.s265876.
3. Brown, C.J.; Simon, T.; Cilibrasi, C.; Lynch, P.J.; Harries, R.W.; Graf, A.A.; Large, M.J.; Ogilvie, S.P.; Salvage, J.P.; Dalton, A.; Giamas, G.; King, A.A.K. Tuneable synthetic reduced graphene oxide scaffolds elicit high levels of three-dimensional glioblastoma interconnectivity *in vitro. J. Mater. Chem. B.* **2022**, *10*, 373-383, https://doi.org/10.1039/D1TB01266E.
4. Hummers Jr., W.S.; Offeman, R. Preparation of graphitic oxide. *J. Am. Chem. Soc.* **1958,** *80*, 1339, https://doi.org/10.1021/ja01539a017.
5. Al-Ruqeishi, M.S.; Mohiuddin, T.; Al-Moqbali, M.; Al-Shukaili, H.; Al-Mamari, S.; Al-Rashdi, H.; Al-Busaidi, R.; Sreepal, V.; Nair, R.R. Graphene Oxide Synthesis: Optimizing the Hummers and Marcano Methods. *Nanoscience and Nanotechnology Letters* **2020,** *12*, 88-95, http://dx.doi.org/10.1166/nnl.2020.3074.
6. Singh, V.; Joung, D.; Zhai, L.; Das, S.; Khondaker, S.I.; Seal, S. Graphene based materials: past, present and future. *Progress in Materials Science* **2011,** *56*, 1178-1271, https://doi.org/10.1016/j.pmatsci.2011.03.003.
7. Beitollahi, H.; Garkani-Nejad, F.; Tajik, S.; Ganjali, M. Voltammetric determination of acetaminophen and tryptophan using a graphite screen printed electrode modified with functionalized graphene oxide nanosheets within a Fe_3O_4@ SiO_2 nanocomposite. *Ir. J. Pharm. Res.* **2019,** *18*, 80-90, https://dx.doi.org/10.22037/ijpr.2019.2326.
8. Ryu, B.D.; Hyung, J.-H.; Han, M.; Ko, K.B.; Park, Y.J.; Cuong, T.V.; Cho, J.; Hong, C.-H. Effect of characteristic properties of graphene oxide on reduced graphene oxide/Si schottky diodes performance. *Materials Science in Semiconductor Processing* **2016**, *44*, 1-7, https://doi.org/10.1016/j.mssp.2015.12.022.
9. Wang, K.; Ruan, J.; Song, H.; Zhang, J.; Wo, Y.; Guo, S.; Cui, D. Biocompatibility of graphene oxide. *Nanoscale Res Lett.* **2011**, *6*, 8, https://doi.org/10.1007/s11671-010-9751-6.
10. Ghulam, A.N.; dos Santos, O.A.; Hazeem, L.; Pizzorno Backx, B.; Bououdina, M.; Bellucci, S. Graphene Oxide (GO) Materials—Applications and Toxicity on Living Organisms and Environment. *J. Funct. Biomater.* **2022,** *13*, 77, https://doi.org/10.3390/jfb13020077.
11. Lin, W.; Huang, Y.-W.; Zhou, X.-D.; Ma, Y. In vitro toxicity of silica nanoparticles in human lung cancer cells. Toxicol Appl Pharmacol. **2006,** *217*, 252-259, https://doi.org/10.1016/j.taap.2006.10.004.
12. Wottrich, R.; Diabaté, S.; Krug, H.F. Biological effects of ultrafine model particles in human macrophages and epithelial cells in mono-and co-culture. *Int. J Hygiene Env. Health* **2004,** *207*, 353-361, https://doi.org/10.1078/1438-4639-00300.
13. Vallet-Regí, M.; Schüth, F.; Lozano, D.; Colilla, M.; Manzano, M. Engineering mesoporous silica nanoparticles for drug delivery: where are we after two decades? *Chem. Soc. Rev.* **2022**, *51*, 5365-5451, https://doi.org/10.1039/D1CS00659B.
14. Li, X.; Wang, Z.; Li, Q.; Ma, J.; Zhu, M. Preparation, characterization, and application of mesoporous silica-grafted graphene oxide for highly selective lead adsorption. *Chem. Eng. J.* **2015,** *273*, 630-637, https://doi.org/10.1016/j.cej.2015.03.104.
15. Theodorakis, N.; Saravanou, S.-F.; Kouli, N.-P.; Iatridi, Z.; Tsitsilianis, C. PH/Thermo-Responsive Grafted Alginate-Based SiO_2 Hybrid Nanocarrier/Hydrogel Drug Delivery Systems. *Polymers* **2021,** *13*, 1228, https://doi.org/10.3390/polym13081228.
16. Pandey, S.K.; Patel, D.K.; Thakur, R.; Mishra, D.P.; Maiti, P.; Haldar, C. Anti-cancer evaluation of quercetin embedded PLA nanoparticles synthesized by emulsified nanoprecipitation. *Int. J Biol. Macromol.* **2015,** *75*, 521-529, https://doi.org/10.1016/j.ijbiomac.2015.02.011.
17. Croitoru, A.-M.; Moroșan, A.; Tihăuan, B.; Oprea, O.; Motelică, L.; Trușcă, R.; Nicoară, A.I.; Popescu, R.-C.; Savu, D.; Mihăiescu, D.; Ficai, A. Novel Graphene Oxide/Quercetin and Graphene Oxide/Juglone

Nanostructured Platforms as Effective Drug Delivery Systems with Biomedical Applications. *Nanomaterials* **2022,** *12*, 1943, https://doi.org/10.3390/nano12111943.
18. Septembre-Malaterre, A.; Boumendjel, A.; Seteyen, A.-L.S.; Boina, C.; Gasque, P.; Guiraud, P.; Sélambarom, J. Focus on the high therapeutic potentials of quercetin and its derivatives. *Phytomedicine Plus* **2022**, *2*, 100220, https://doi.org/10.1016/j.phyplu.2022.100220.
19. Khursheed, R.; Singh, S.K.; Wadhwa, S.; Gulati, M.; Awasthi, A. Enhancing the potential preclinical and clinical benefits of quercetin through novel drug delivery systems. *Drug Discov. Today* **2020,** *25*, 209-222, https://doi.org/10.1016/j.drudis.2019.11.001.
20. Khursheed, R.; Singh, S.K.; Wadhwa, S.; Gulati, M.; Kapoor, B.; Jain, S.K.; Gowthamarajan, K.; Zacconi, F.; Chellappan, D.K.; Gupta, G.; Jha, N.K.; Gupta, P.K.; Dua, K. Development of mushroom polysaccharide and probiotics based solid self-nanoemulsifying drug delivery system loaded with curcumin and quercetin to improve their dissolution rate and permeability: State of the art. *Int. J. Biol Macromol.* **2021,** *189*, 744-757, https://doi.org/10.1016/j.ijbiomac.2021.08.170.
21. Zaaba, N.; Foo, K.; Hashim, U.; Tan, S.; Liu, W.-W.; Voon, C.H. Synthesis of graphene oxide using modified hummers method: solvent influence. *Procedia Engineering* **2017,** *184*, 469-477, https://doi.org/10.1016/j.proeng.2017.04.118.
22. Stankovich, S.; Dikin, D.A.; Piner, R.D.; Kohlhaas, K.A.; Kleinhammes, A.; Jia, Y.; Wu, Y.; Nguyen, S.T.; Ruoff, R.S. Synthesis of graphene-based nanosheets via chemical reduction of exfoliated graphite oxide. *Carbon* **2007,** *45*, 1558-1565, https://doi.org/10.1016/j.carbon.2007.02.034.
23. Catauro, M.; Papale, F.; Bollino, F.; Piccolella, S.; Marciano, S.; Nocera, P.; Pacifico, S. Silica/quercetin sol–gel hybrids as antioxidant dental implant materials. *Sci. Tech. Adv. Mater.* **2015**, *16*, 035001, https://doi.org/10.1088/1468-6996/16/3/035001.
24. Azadi, S.; Sardarian, A.R.; Esmaeilpour, M. Magnetically-recoverable Schiff base complex of Pd (II) immobilized on Fe_3O_4@ SiO_2 nanoparticles: an efficient catalyst for the reduction of aromatic nitro compounds to aniline derivatives. *Monatshefte fuer Chemie - Chem. Monthly* **2021,** *152*, 809-821, http://dx.doi.org/10.1007/s00706-021-02787-7.
25. Kazemi, S.; Pourmadadi, M.; Yazdian, F.; Ghadami, A. The synthesis and characterization of targeted delivery curcumin using chitosan-magnetite-reduced graphene oxide as nanocarrier. *Int. J Biol. Macromol.* **2021,** *186*, 554-562, https://doi.org/10.1016/j.ijbiomac.2021.06.184.
26. Hanh, N.T.; Xuyen, N.T.; Thuy, T.T.T. Synthesis and characterization of Fe_3O_4/GO nanocomposite for drug carrier. *Viet. J. Chem.* **2018,** *56*, 642-646, http://dx.doi.org/10.1002/vjch.201800063.
27. Lu, Q.; Wang, Z.; Li, J.; Wang, P.; Ye, X. Structure and photoluminescent properties of ZnO encapsulated in mesoporous silica SBA-15 fabricated by two-solvent strategy. *Nanoscale Res. Lett.* **2009,** *4*, 646, https://doi.org/10.1007/s11671-009-9294-x.
28. Su, Y.-l. Preparation of polydiacetylene/silica nanocomposite for use as a chemosensor. *React. Funct. Polym.* **2006,** *66*, 967-973, https://doi.org/10.1016/j.reactfunctpolym.2006.01.021.
29. Xu, Z.; Bando, Y.; Liu, L.; Wang, W.; Bai, X.; Golberg, D. Electrical conductivity, chemistry, and bonding alternations under graphene oxide to graphene transition as revealed by in situ TEM. *ACS Nano* **2011,** *5*, 4401-4406, https://doi.org/10.1021/nn103200t.
30. Rades, S.; Hodoroaba, V.-D.; Salge, T.; Wirth, T.; Lobera, M.P.; Labrador, R.H.; Natte, K.; Behnke, T.; Gross, T.; Unger, W.E.S. High-resolution imaging with SEM/T-SEM, EDX and SAM as a combined methodical approach for morphological and elemental analyses of single engineered nanoparticles. *RSC Advances* **2014,** *4*, 49577-49587, https://doi.org/10.1039/C4RA05092D.
31. Veisi, H.; Tamoradi, T.; Karmakar, B.; Mohammadi, P.; Hemmati, S. In situ biogenic synthesis of Pd nanoparticles over reduced graphene oxide by using a plant extract (*Thymbra spicata*) and its catalytic evaluation towards cyanation of aryl halides. *Mat. Sci. Eng: C* **2019,** *104*, 109919, https://doi.org/10.1016/j.msec.2019.109919.
32. Saipanya, S.; Waenkaew, P.; Maturost, S.; Pongpichayakul, N.; Promsawan, N.; Kuimalee, S.; Namsar, O.; Income, K.; Kuntalue, B.; Themsirimongkon, S.; Jakmunee, J. Catalyst Composites of Palladium and N-Doped Carbon Quantum Dots-Decorated Silica and Reduced Graphene Oxide for Enhancement of Direct Formic Acid Fuel Cells. *ACS Omega* **2022**, *7*, 17741-17755, https://doi.org/10.1021/acsomega.2c00906.
33. Webb, B.A.; Chimenti, M.; Jacobson, M.P.; Barber, D. Dysregulated pH: a perfect storm for cancer progression. *Nature Reviews Cancer* **2011,** *11*, 671-677, https://doi.org/10.1038/nrc3110.
34. Steffi, A.P.; Balaji, R.; Chandrasekar, N.; Prakash, N.; Rajesh, T.P.; Ethiraj, S.; Samuel, M.S.; Vuppala, S., High-performance anti-corrosive coatings based on rGO-SiO_2-TiO_2 ternary heterojunction nanocomposites

for superior protection for mild steel specimens. *Diamond and Related Materials* **2022,** *125*, 108968, https://doi.org/10.1016/j.diamond.2022.108968.